nanomaterials

MDPI

# Supplementary Materials

# Effect of Platinum Content on Properties of CNT-Supported Pt–Mo Catalyst for Ethanol Electrooxidation Reaction

**Oleg Korchagin [1,2,*], Marina Radina [1], Alexey Kuzov [1], Vladimir Andreev [1,2] and Andzhela Bulanova [2]**

[1] Frumkin Institute of Physical Chemistry and Electrochemistry, Russian Academy of Sciences, Moscow 119071, Russia; merenkovamarina@mail.ru (M.R.); scourge@mail.ru (A.K.); vandr@phyche.ac.ru (V.A.)

[2] Department of Physical Chemistry and Chromatography, Samara University, Samara 443086, Russia; av.bul@yandex.ru

* Correspondence: oleg-kor83@mail.ru

To evaluate possible changes in the support (CNT) structure as a result of the catalyst synthesis, the specimens were studied using the Raman spectroscopy. The Raman spectra were recorded in the backscatter mode using an InVia Renishaw spectrometer (ZEISS, Germany) equipped with a detector with a charged-coupled device (CCD), an ionic laser ($\lambda$ = 532 nm), and a grating with a resolution of 1800 lines/mm with a spectral resolution of 1 $cm^{-1}$.

As shown in Figure S1, the spectra of all specimens exhibit three peaks characteristic of carbon materials: the D band of disordered carbon (~1350 $cm^{-1}$), the peak G of graphi-tized carbon (~ 1580 $cm^{-1}$) and 2D peak (~ 2690 $cm^{-1}$) [1]. The D band indicates the presence of structural defects and the ID/IG intensity ratio enables us to estimate a degree of mate-rial disorder. As is seen from Table S1, a degree of disorder increases upon passing from CNT to the catalysts, although no direct correlation is observed between the catalyst com-position and the $I_D/I_G$ parameter. No noticeable shift of the D and G bands is observed during the catalyst formation. This indicates that the carbon support structure is retained, which is consistent with the SEM images.

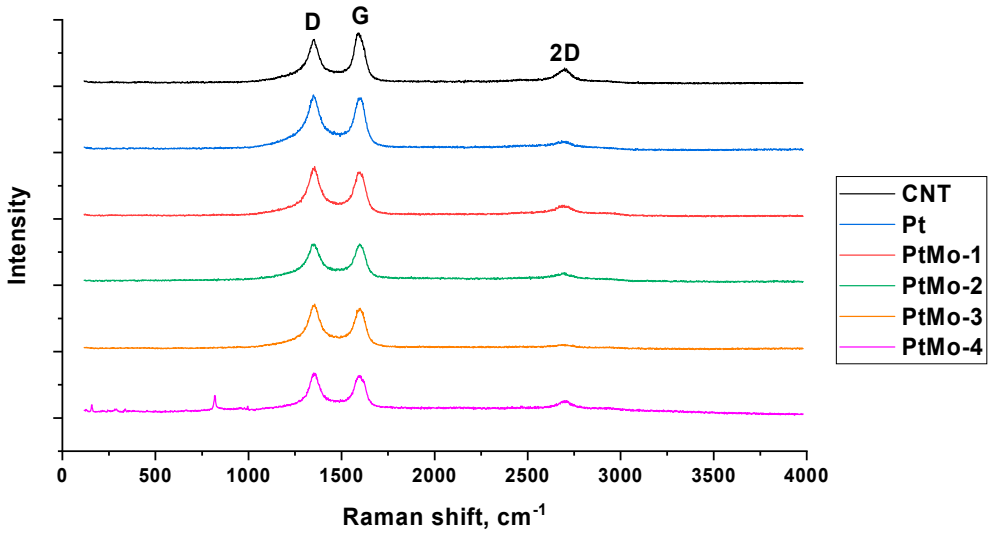



**Figure S1.** Raman spectra for test materials.

**Table S1.** Characteristics of test materials according to the Raman spectroscopy data.

| Material | D, $cm^{-1}$ | G, $cm^{-1}$ | 2D, $cm^{-1}$ | $I_D$ | $I_G$ | $I_{2D}$ | $I_D/I_G$ | $I_{2D}/I_G$ |
|---|---|---|---|---|---|---|---|---|
| CNT | 1353 | 1594 | 2698 | 1414 | 1603 | 549 | 0.88 | 0.340 |
| Pt | 1349 | 1599 | 2703 | 1735 | 1644 | 335 | 1.06 | 0.204 |
| PtMo-1 | 1355 | 1601 | 2697 | 1580 | 1416 | 417 | 1.12 | 0.290 |
| PtMo-2 | 1353 | 1597 | 2698 | 1246 | 1247 | 383 | 1.01 | 0.307 |
| PtMo-3 | 1355 | 1600 | 2701 | 1437 | 1304 | 218 | 1.10 | 0.167 |
| PtMo-4 | 1351 | 1599 | 2707 | 1359 | 1284 | 526 | 1.06 | 0.410 |

1. Lilloja, J.; Kibena-Põldsepp, E.; Sarapuu, A.; Kikas, A.; Kisand, V.; Käärik, M.; Merisalu, M.; Treshchalov, A.; Leis, J.; Sammelselg, V.; et al. Nitrogen-Doped Carbide-Derived Carbon/Carbon Nanotube Composites as Cathode Catalysts for Anion Exchange Membrane Fuel Cell Application. *Appl. Catal. B Environ.* **2020**, *272*, 119012, doi:10.1016/j.apcatb.2020.119012.